Correlation-based Radio Localization in an Indoor Environment

Thomas Callaghan, Nicolai Czink, Francesco Mani, Arogyaswami Paulraj, George Papanicolaou

Abstract

We investigate the feasibility of using correlation-based methods for estimating the spatial location of distributed receiving nodes in an indoor environment. Our algorithms do not assume any knowledge regarding the transmitter locations or the transmitted signal, but do assume that there are ambient signal sources whose location and properties are, however, not known.

The key idea is to compute pairwise cross correlations of the signals received at the nodes and use them to estimate the travel time between these nodes. If the ambient signal sources have sufficient space-time diversity, then the cross correlations recover the distance between the two receiving nodes. By doing this for all pairs of receivers we can construct an approximate map of their location using multidimensional scaling methods.

We test this localization algorithm in a cubicle-style office environment based on both ray-tracing simulations, and measurement data from a radio measurement campaign using the Stanford broadband channel sounder. Contrary to what is seen in other applications of cross-correlation methods, the strongly scattering nature of the indoor environment complicates distance estimation. However, using statistical methods, the rich multipath environment can be turned partially into an advantage by enhancing ambient signal diversity and therefore making distance estimation more robust.

The main result is that with our correlation-based statistical estimation procedure applied to the real data, assisted by multidimensional scaling, we were able to compute spatial antenna locations with an average error of about 2 meters and pairwise distance estimates with an average error of 2.33 meters. The theoretical resolution limit for the distance estimates is 1.25 meters.

Part of this work was supported by US Army grant W911NF-07-2-0027-1, by AFOSR grant FA9550-08-1-0089, by the Austria Science Fund (FWF) through grant NFN SISE (S10607). FTW is supported by the Austrian Government and by the City of Vienna within the competence center program COMET.

Index Terms

indoor localization; sensor networks; signal correlations; rich scattering; multidimensional scaling

I. Introduction

Indoor localization is a long-standing open problem in wireless communications [1], particularly in wireless sensor networks [2], [3]. Localization techniques in non-line-of-sight indoor environments face two major challenges: (i) multipath from rich scattering makes it difficult to identify the direct path, limiting thus the use of distance estimation based on time-delay-of-arrival (TDOA) methods; (ii) the strongly changing propagation loss due to shadowing impairs distance estimation based on the received signal strength (RSS).

In both kinds of algorithms, TDOA and RSS, nodes can estimate their own location relative to several "anchor nodes" acting as transmitters. This is commonly done by estimating the distances to the anchor nodes and subsequently using triangularization for position estimation.

The estimation of the TDOA is done either by round-trip time estimation [4], the transmission of specific training sequences [5], or simply by detecting the first peak of the received signal [6]. Ultra-wide band communications are specifically suited for TDOA distance estimation because of the large available bandwidth [7].

Many publications discuss RSS-based distance estimation. The work presented in [8] provides a comprehensive overview of an actual implementation using WiFi hotspots in a self-configuring network.

Another technique described in [9] is using spatial signatures for localization. However, this requires multiple antennas at the nodes and a database of spatial locations. Moreover, this technique is bound to specific antenna requirements.

Correlation-based methods [10] have been widely used for many years in a variety of fields, including sensor networks. Some examples include estimation of the speed of seismic waves and even earth-quake prediction [11]. The idea there is to cross correlate seismic noise signals from sensors deployed in a wide area so as to estimate the travel time of the seismic waves from one sensor to the other. Given the sensor locations, the wave speed can be estimated using travel time tomography.

Contribution We investigate here the feasibility of *passive, correlation-based indoor radio localization*. In contrast to the previous works, we consider both the source positions and the

source signals to be unknown. We just require that there are ambient signals present. The receiving nodes estimate their distances to other nodes in a three step procedure: (i) first, all nodes are receiving and storing ambient signals, (ii) the nodes communicate their received signals to other nodes, (iii) the nodes estimate the pairwise distances between them by cross correlating their received signals and identifying peaks in the cross-correlation function. If the ambient signals have sufficient spatial diversity, then the peaks of the cross correlations provide a robust estimate of the distance between the two receiving antennas. By doing this for all pairs of receiving nodes, we construct an approximate map of their locations using weighted least squares methods, in particular multidimensional scaling (MDS) [12], [13].

We quantify the performance of the algorithms in an indoor environment with both ray-tracing simulations and data from a recently conducted radio measurement campaign, using the RUSK Stanford multi-antenna radio channel sounder with a center frequency of 2.45 GHz and bandwidth of 240 MHz [14].

The strongly scattering nature of the indoor environment makes the pairwise distance estimation challenging. However, in contrast to other localization methods, multipath from rich scattering is now both helpful and harmful for distance estimation. While multipath increases spatial diversity, it also leads to additional peaks in the correlation function. The main feature in this work is the proper treatment and utilization of the beneficial properties of rich multipath while controlling its negative effects. To achieve this goal, we propose statistical peak-selection algorithms that significantly increases the localization accuracy.

We demonstrate, therefore, that passive, correlation-based radio localization is feasible in wireless indoor environments.

Organization The paper is organized as follows. Section II provides a brief motivation for using correlation-based methods for distance estimation. In Section III we consider the problem of travel time estimation using cross correlations. Section IV presents different approaches for improving the pairwise travel-time estimation based on correlation-based methods. Section V briefly presents how we use MDS to find position estimates, discusses the results from applying our algorithms and MDS to the simulated and measured data, and demonstrates the effect of transmitter positions using the simulated data. With Section VII we conclude the paper. Appendices A and B provide brief descriptions of the ray-tracing simulations and the measurement data we use in this paper.

II. Motivation for the use of Cross Correlations in distance estimation

We start out with a simple example. Consider a line-of-sight environment, as shown in Figure 1. A single source emits a pulse $s(\tau) = \delta(\tau)$, while two receivers record the signals $r_1(\tau)$ and $r_2(\tau)$, respectively, where τ denotes the delay and $\delta(\cdot)$ denotes the Dirac delta function. The positions of the source and of the receivers are unknown. The signal emitted by the source is received by both receivers with certain delay lags. Thus, the received signals become $r_1(\tau) = \gamma_1\delta(\tau - \tau_1)$, and $r_2(\tau) = \gamma_2\delta(\tau - \tau_2)$, where τ_k denotes the delay lag from the source to the kth receiver, and γ_k denotes the path loss of the signal. By cross correlating the two received signals,

$$c_{1,2}(\tau) = \int r_1(\tau')r_2(\tau + \tau')\mathrm{d}\tau' = \gamma_1\gamma_2\delta(\tau - (\tau_1 - \tau_2)), \tag{1}$$

we see that the resulting cross correlation is a pulse at the delay difference $\Delta\tau = \tau_1 - \tau_2$. This also holds for arbitrary source signals, as long as they have certain auto-correlation properties, as shown in the next section.

By finding the peak in the received signals cross correlation, we can estimate the distance between the receivers as $\hat{d} = \Delta\tau\, c_0$, with c_0 indicating the speed of light. When the transmitter is on a straight line going through the two receivers, this estimated distance is the exact distance between the nodes [10]. However, when there is an angle α between the direction of the plane wave front and the straight line between the receivers, the distance estimate will give $\hat{d} = d\,|\cos(\alpha)|$, which carries a systematic error.

Since we do not know the position of the source, we cannot correct for this systematic error, but we can quantify its distribution. For this we make the following assumptions: (i) we consider horizontal wave propagation only, since it is predominant in indoor environments; (ii) all directions of the transmitted signals are equally likely, i.e. α is distributed uniformly, $\alpha \sim \mathcal{U}[-\pi, \pi)$. So, we can calculate the probability density function of the estimated distance, $p_{\hat{d}}(\hat{d})$ by transformation of the random variable α as

$$p_{\hat{d}}(\hat{d}) = \begin{cases} \frac{2}{\pi}\frac{1}{d\sqrt{1-(\hat{d}/d)^2}} & \dots \quad 0 \le \hat{d} \le d, \\ 0 & \dots \quad \hat{d} > d, \end{cases} \tag{2}$$

and also obtain its cumulative distribution function

$$F(\hat{d}) = \frac{2}{\pi}\arcsin\left(\frac{\hat{d}}{d}\right) \quad \dots \; 0 \le \hat{d} \le d, \tag{3}$$

which is shown in Figure 2. It turns out that in 50% of all cases, our distance estimation error is less than 30% (indicated by the dashed lines).

While basing the distance estimation on a single plane wave is questionable because of the rather large systematic error, real radio propagation environments provide diversity by multiple sources and by multipath. The receiver cross correlation will therefore have multiple peaks, which provide more information about the propagation environment, which improves distance estimation. The way to exploit this signal diversity and how to obtain a robust distance estimate is the topic of the rest of this paper.

To provide another motivation as to why cross correlations can be used for travel time estimation, we'll briefly review results for cross correlations in a homogeneous environment [10], [15], [16]. Let $r_1(t)$ and $r_2(t)$ denote the time-dependent wave fields recorded by two sensors at $\mathbf{x}_1$ and $\mathbf{x}_2$. Their cross correlation function over the time interval $[0, T]$ with time lag τ is given by

$$c_{1,2}(\tau) = \frac{1}{T}\int_0^T r_1(t) r_2(t+\tau)\mathrm{d}t$$

In the case of a 3-D homogeneous medium with spatially uniform noise source distribution, the field at each receiver can be decomposed as a superposition of uncorrelated plane waves from various directions. It has been established that the normalized cross-spectral density $c_{1,2}(\omega)$ at frequency ω between two sensors $\mathbf{x}_1$ and $\mathbf{x}_2$ separated by r is $c_{1,2}(\omega) = [\sin(\omega r/c)]/(\omega r/c)$. In the time domain, the normalized correlation function is

$$\begin{aligned} c_{1,2}(\tau) &= \frac{1}{2\pi}\int_{-\infty}^{\infty} c_{1,2}(\omega) e^{j\omega\tau}\mathrm{d}\omega \\ &= \frac{1}{4\pi}\int_{-\infty}^{\infty}\left[\frac{e^{j\omega(\tau+r/c)}}{j\omega r/c} - \frac{e^{j\omega(\tau-r/c)}}{j\omega r/c}\right]\mathrm{d}\omega \end{aligned}$$

The time derivative of the cross correlation function is

$$\frac{d}{d\tau}c_{1,2}(\tau) = \frac{1}{4\pi r/c}\left[\delta(\tau + r/c) - \delta(\tau - r/c)\right].$$

These two terms correspond to the forward and backward (symmetrized in time)impulse response function between the two receivers. From the peaks of these functions, one can deduce the travel time between sensors $\mathbf{x}_1$ and $\mathbf{x}_2$. This result has been shown to extend to scattering media as well [10], where the delta functions on the right are replaced by the time dependent Green's function (channel transfer function) between the two receivers.

Based on this motivation, the theory indicates that the peak of the derivative of the cross correlation function is a good estimate of the travel time. However, due to the strongly scattering medium, the cross correlation is not smooth and has many peaks making the derivative computation unreliable. Instead we use the other motivation and use the peaks from the cross correlation function to estimate the travel time (and distance).

III. Computation of Cross Correlations

This section describes the computation of the cross correlations using a more complex setting with multiple sources, including scattering in the environment. A finite number of L sources, S_l, $l = 1 \dots L$, transmit random uncorrelated signals $s_l(t, \tau)$, i.e.

$$\mathrm{E}\left\{s_l(t,\tau)s_{l'}(t',\tau')\right\} = \begin{cases} 1 & \dots \quad l = l' \ \wedge \tau = \tau' \\ 0 & \dots \quad l \neq l' \ \vee \ \tau \neq \tau', \end{cases}$$

where t denotes absolute time (assuming block transmission), and τ denotes the delay lag. For example, white noise signals fulfill these properties asymptotically, when $\tau \to \infty$. We assume that the channel stays constant within the transmission of a block and then changes due to fading. A number of K receivers, R_k, $k = 1 \dots K$, records their respective received signals $r_k(t, \tau)$ from these multiple random sources, i.e.

$$r_k(t,\tau) = \sum_{l=1}^{L} \int_{\tau'} s_l(t,\tau') h_{kl}(t, \tau - \tau') \mathrm{d}\tau', \tag{4}$$

where $h_{kl}(t, \tau)$ denotes the time and frequency selective radio channel from the lth source to the kth receiver.

The cross correlation function (CCF) between two received signals at time t is

$$c_{k,k'}(t,\tau) = \int_{\tau'} r_k(t,\tau') r_{k'}(t, \tau + \tau') \mathrm{d}\tau', \tag{5}$$

which can be written as

$$c_{k,k'}(t,\tau) = \sum_{l=1}^{L} \int_{\tau'} h_{kl}(t,\tau') h_{k'l}(t, \tau + \tau') \mathrm{d}\tau', \tag{6}$$

when the source signals fulfill the condition in (4). This CCF provides information about the delay lag between the two receivers R_k and $R_{k'}$ as discussed in the previous section.

When applying this method to radio channel measurements, the CCF can be averaged over all measured time instants T (i.e. averaging over fading variations of the channel) by

$$\hat{c}_{k,k'}(\tau) = \frac{1}{T}\sum_{t=1}^{T} c_{k,k'}(t,\tau). \tag{7}$$

For the actual implementation, all convolutions and correlations in delay domain are implemented as multiplications in frequency domain.

It is well known [10] that for an infinite number of (uncorrelated) orthogonal sources, spatially distributed uniformly over all solid angles in 3-D, the resulting CCF has a rectangular shape, centered at zero and having a width of $2d/c_0$. Since in our simultaions and measurements (cf. Appendices A and B) only a finite number of transmitting antennas contribute to the signal recorded at each receiving antenna, we rely on sufficient scattering in the medium for enhancement of directional diversity. This leads to a trade-off between two effects: (i) Multipath increases the signal diversity and thus creates peaks in the CCF that better represent the true distance, but (ii) multipath also generates ”wrong” (additional) peaks from propagation paths that do not directly travel through the receivers, which in turn reduce the accuracy of distance estimation.

An example of a CCF evaluated from our measurements (cf. Appendix B) is shown in Figure 3. We observed a strong directionality of the impinging radio waves, which leads to peaks at various distances. The true distance of $4.9\,\mathrm{m}$, indicated by the dashed lines, is clearly visible as a peak in the CCF. However, other strong peaks are also present. Because of these multiple peaks, which sometimes dwarf the accurate peaks, a more elaborate distance estimation method is necessary.

IV. Improved distance estimation method

The distance estimation can be improved in by combining three ideas: (i) using short-time estimates of the CCF, (ii) using multiple peaks from the CCF for distance estimation, and (iii) using relative weighting on the peaks from the CCF to distinguish between peaks of comparable height (power).

A. Short-time estimates of the CCF

The long-time averaging applied in the original approach in (7) may reduce information about the propagation environment. By using the short-time estimates of the CCF from (5), individual

differences in the propagation environment, caused by fading, can be utilized to improve the distance estimation as follows.

B. Multiple peaks for distance estimation

As motivated in Section II, the distance between two receivers is proportional to the propagation delay,

$$\hat{d}_{k,k'} = \hat{\tau}_{k,k'}\, c_0, \tag{8}$$

where $\hat{d}_{k,k'}$ and $\hat{\tau}_{k,k'}$ denote the distance estimate and travel time estimate, respectively.

A direct way to estimate the delay between two receivers is to identify the largest peak in their CCF. This approach does not perform well in multipath environments. Instead, we consider a more robust statistical approach based on *multiple peaks* in the CCF. The problem is how to choose and how to use the peaks in the CCF.

We use a statistical approach as follows: the CCF is sorted according to

$$\hat{c}_{k,k'}(t,\tau_1) > \hat{c}_{k,k'}(t,\tau_2) > \cdots > \hat{c}_{k,k'}(t,\tau_M), \tag{9}$$

with M denoting the number of resolved delays in the CCF. From this sorting, we use $p = 0.5\%$ of the delays having the strongest CCF values, i.e.

$$\hat{\tau}_{k,k'}(t,n) = |\tau_n|, \quad n \in [1,\ldots,\lfloor pM \rfloor], \tag{10}$$

which corresponds to taking the top 4 peaks in our data set.

We then take a weighted average of these multiple delays as the distance estimate, i.e.

$$\hat{\tau}_{k,k'} = \frac{1}{T \cdot \lfloor pM \rfloor} \sum_{t=1}^{T} \sum_{n=1}^{\lfloor pM \rfloor} w_{k,k'}(t,n)\hat{\tau}_{k,k'}(t,n), \tag{11}$$

where the choice of the weights $w_{k,k'}(t,n)$ is described in the next section.

C. Cross-Correlations with weights

To improve the distance estimation further, we propose to distinguish between dominant peaks and peaks of similar amplitude. For this reason, we weigh the peaks based on their relative amplitude.

Since we are using $N = \lfloor pM \rfloor$ peaks, we assigned a weight to each peak equal to the ratio between its amplitude over the Nth largest peak's amplitude,

$$w_{k,k'}(t,n) = \hat{c}_{k,k'}(t,\tau_n)/\hat{c}_{k,k'}(t,\tau_N), \quad n \in [1,N]. \tag{12}$$

The estimates computed by this statistical procedure can subsequently be improved by taking geometrical considerations into account as shown in the next section.

V. RESULTS

In the subsections that follow, we apply these distance estimation methods to both a simulated dataset and data from an indoor radio channel measurement campaign. In addition to distance estimation results, we also present localization results as estimated receiver positions are also of much interest in this problem. To estimate positions from pairwise distance estimates between all receivers, it is natural to use multidimensional scaling (MDS) algorithms. These statistical techniques, that date back 50 years, take as its input a set of pairwise similarities and assign them locations in space [12], [13]. Recently, it was applied to a different, but related problem, of node localization in sensor networks [3].

In MDS we solve the following least-squares optimization problem

$$\min_{\{\mathsf{R}_k\}} \sum_{k \neq k'} \lambda_{k,k'} \left| \hat{d}_{k,k'} - ||\mathsf{R}_k - \mathsf{R}_{k'}||_2 \right|^2, \tag{13}$$

where $\hat{d}_{k,k'}$ are the provided distance estimates, $\lambda_{k,k'}$ are weights, $||\cdot||_2$ is the Euclidean distance, and $\{\mathsf{R}_k\}$ is the set of locations of the receivers $\{R_k\}$. In our problem we assume the locations to lie in $\mathbb{R}^2$. As we will show in the next section, the error in our pairwise distance estimates is correlated to the distance estimates themselves. Thus, a natural weighting is $\lambda_{k,k'} = 1/\hat{d}^{\alpha}_{k,k'}$, for $\alpha \geq 0$. We found that $\alpha = 1$ produced the smallest error. To solve this optimization problem, we used the algorithm given in [17], which resulted in the final position estimates $\{\mathsf{R}_k\}$ of the receivers. The results from solving this optimization problem are sensitive to the initial guess, so we used the procedure to compute our initial position estimate in [18].

A. Ray-tracing simulations

We first present our localization method applied to a environment simulated using a state-of-the-art ray-tracing tool including diffuse scattering. A detailed description of the ray tracing

algorithm is provided in Appendix A. The nodes were set up as shown in Figure 4. We *estimated the distance* between all pairs of nodes and calculated the distance estimation error using the ("statistical peak selection") method presented in Section IV. As reference to with which to compare we use the long-time average peak method ("cumulative peak"), i.e. selecting the strongest peak out of the averaged long-time CCF given in (7).

A scatter plot of the true distance versus the estimated distance for these approaches is shown in Figure 5. This plot exhibits a significant underestimation bias. We expect this from the theory, especially when we have strong sources illuminating from the "wrong" angle.

The empirical cdfs of the distance estimation errors are shown by the dashed lines in Figure 6. Using only the peak of the averaged long-time CCF performs worst, by far, because it does not use the diversity in time. In contrast, using our statistical peak selections, significantly lowers the distance estimation error.

With the simulated channel bandwidth of 240 MHz, our theoretical resolution is limited to an accuracy of $c/B = 1.25$ meters. Our final results produced an average pairwise distance estimation error of 4.55 meters.

Next, we used MDS to obtain position estimates. By the weights introduced in the MDS[1], we make use of the correlation between the distance estimation and its error. In Figure 7, the localization results using our statistical method are shown. The true locations are denoted by circles, while the estimated locations are marked by squares. The arrows are connecting the estimates to their respective true locations.

Looking at this figure, we notice that the error is mostly in the x-direction. The reason for this is the strong directionality of the waves coming mostly from top/bottom, but not from left/right. This naturally leads to an underestimation of the distance between the horizontally-spaced node pairs. We also observe that the receiving antennas that are lying centrally have the smallest position estimation errors. This is due to the increased diversity of the source signals. We find an average position estimation error of 3.66 m, with a minimum error of 1.25 m, a maximum error of 5.87 m, and a standard deviation of 1.56 m.

Looking at the position estimates when using only the long-time average peak in Figure 8, the results seem questionable. Some distances are strongly underestimated as already seen

[1]These weights are not to be confused with the weighting of the peaks

in Figure 5. In this approach, reliable position estimation becomes impossible. This clearly demonstrates that multipath must not be ignored, but needs to be utilized to enable acceptable distance estimation.

B. Effect of Transmitter Locations

As mentioned earlier, the locations of the transmitters have a great effect on the quality of the distance and position estimation. With our simulated data, we can actually turn off and on certain transmitters and examine the effect that this has. Figure 9 demonstrates that selecting different sets of transmitters produce very different results. These figures use four different sets of transmitters: all, top and bottom, left and right, and the configuration that gave the minimal average position error in a thorough but not exhaustive search.

As expected, using the top and bottom transmitters results in good location estimation in the y-direction while using the left and right transmitters gives good location estimation in the x direction. Comparing the location estimates of the top left and bottom right scatterers in Figure 9d to their position estimates using all of the transmitters (plot (a) in the same figure), one can observe that including the transmitter closest to the true receiver location results in that receiver's estimated position error being larger. This is also consistent with the intuition brought forward in Section II. Sources close to the receiver nodes will most likely lead to an underestimation of the distance.

C. Performance in a Measured Environment

As a proof of concept, we applied our localization method to an indoor radio channel measurement described in Appendix B. The nodes were set up in two squares as shown in Figure 10. As with the ray tracing simulations, we estimated the distance between all pairs of nodes using the ("statistical peak selection") method presented in Section IV. As reference to with which to compare we use the long-time average peak method ("cumulative peak"), i.e. selecting the strongest peak out of the averaged long-time CCF given in (7).

A scatter plot of the true distance versus the estimated distance for these approaches is shown in Figure 11. The interesting fact noted here is that for larger true distances, the distance estimation error becomes larger. This effect can be easily explained by the underlying wave propagation: our approach needs strong waves traveling through the receiver pair. When the receivers are far

apart, the probability of a direct wave from one to the other becomes much lower. This is also the reason why the long-time average peak method performs so badly. The distance between the nodes is strongly underestimated. Only when making use of fading, i.e. diversity in time, the distance estimates become reliable. It is important to note that this result is significantly different than the result with the simulated data. This is due to the fact that the real measurements capture more of the complexity of the rich scattering channel.

Again, the empirical cdfs of the distance estimation errors are shown by the dashed lines in Figure 12. With the measurement bandwidth of 240 MHz, our theoretical resolution is limited to an accuracy of $c/B = 1.25$ meters. Our final results produced an average pairwise distance estimation error of 2.33 meters. Moreover, the distance estimation errors of almost half of our 28 receiving antenna pairs were below the resolution limit, which is again an effect of using the diversity offered by the time variations in the channel.

We also present the results of the *location estimation* in Figure 13. The true locations are denoted by circles, while the estimated locations are marked by squares. The arrows are connecting the estimates to their respective true locations.

Looking at the quadrangle of the bottom four nodes, we observe that the estimates are placed in a rhomboid. The reason for this is the strong directionality of the waves coming mostly from left/right, but not from top/bottom. This naturally leads to an underestimation of the distance between the vertically-spaced node pairs. The result is that the nodes appear squeezed in the y-direction, but do have the correct distance in the x-direction. We also observe that the receiving antennas that are lying centrally have the smallest position estimation errors. This is due to the increased diversity of the source signals. We find an average position estimation error of 2.1 m, with a minimum error of 0.4 m, a maximum error of 3.36 m, and a standard deviation of 0.92 m. The results are similar when using the multi-peak mean method without peak weighting.

As before, when using only the long-time average peak in Figure 14, the results are inaccurate and unreasonable.

VI. Implementation

A realistic implementation of these methods would of course require the consideration of several practical issues, including timing synchronization and information exchange between the

receiver nodes, and optimal selection of the radio band for providing enough ambient signal strength.

Many of these issues can be resolved if we assume that we have a master node with which all receiver nodes can communicate so as to transfer their recorded data. Finally, the master node performs all the calculations, and also ensures the synchronization between the nodes [19].

As for all delay-based localization algorithms, the receiving nodes need to sample the ambient signals with a high sampling rate (and thus bandwidth) using a fast analog-to-digital converter. The advantage of our approach is that the sampling can be done with a low bit resolution, against which our approach is quite robust. Of course, the recorded data can be further compressed before sending it on to the master. Thus, only a limited amount of data needs to be transmitted, leading to a much smaller necessary bandwidth than what was needed for sampling the signal.

VII. Conclusions

In this paper we consider the feasibility of radio localization in a rich-scattering indoor environment using correlation-based techniques.

We presented a systematic way to use peaks in the cross correlations of the received signals for computing pairwise distance estimates and spatial location estimates for a passive network of wireless receiving nodes (sensors). The robustness of the estimation is enhanced by multipath due to scattering but its accuracy is diminished by it. The increased signal diversity improves the estimation robustness, while generating many peaks in the cross correlations. To enhance inter receiver (sensor) distance estimation, we consider utilize statistical methods that utilize multipath effects by taking into account multiple fading realizations of the channel.

We demonstrated the feasibility of our approach using both simulated and real measurements in a cubicle-style office environment. In our simulations, we use a 3-D ray-tracing tool, operating at 2.45 GHz, to measure the radio channels between 14 transmitters and 14 receivers in a simulated cubical office environment with diffuse scattering. In the real measurements, the radio channels between eight transmitters and eight receivers were measured using the RUSK Stanford channel sounder, operating at 2.45 GHz with a bandwidth of 240 MHz. The experimental equipment is special and favors our localization approach. Realistic implementation would require several practical aspects to be considered. Most importantly, a master node would be necessary to

centralize the computation and synchronize the receiver nodes. However, using our equipment, we have demonstrated the feasibility of correlation-based radio localization techniques.

Despite the lack of a large number of transmitting antennas, we were able utilize the spatial diversity of the strongly scattering room by using our improved estimation methods. The main result is that with the real data we were able to estimate spatial antenna locations with less than 2 meters error when the theoretical resolution limit is 1.25 meters.

APPENDIX

A. Ray-tracing Simulations

Ray-Tracing (RT) is a site-specific geometrical technique that evaluates propagation paths followed by rays as they interact with the environment. A key feature of indoor propagation channels is diffuse scattering. For this reason, a classic 3-D RT tool [20], improved with penetration and diffuse scattering [21], has been used in this work to model the channel. The model of diffuse scattering is described in [22]. A geometrical description of the environment, frequency, number of interactions and dielectric properties of materials are some of the input parameters of a RT tool. In the following sections the ones used in this work are presented.

1) Setup Parameters: The simulation frequency has been set to 2.45 GHz. Antenna radiation patterns are the ones of vertically polarized dipoles both at receive (Rx) and source/transmit (Tx) side. Whenever Tx are placed at walls, they radiate only into the relative half-space. A maximum of three reflections, single diffraction and single-bounce scattering has been used in the simulations. A directive scattering pattern model with scattering coefficient $S = 0.4$ and beamwidth $\alpha_r = 4$ has been chosen. These paths were filtered using a rectangular filter in frequency domain with a bandwidth of 240 MHz to resemble the measurements.

2) Simulated Environment: A cubicle-style office scenario has been used as input for the RT tool. The dimensions of the room have been set to 50 m $\times$ 20 m with a height of 4 m. The walls, the ceiling and the floor are supposed to be made of concrete. Cubicles are 4 m $\times$ 3 m $\times$ 1.8 m, and are organized in two rows. Cubicles are represented by their metallic frames that have been treated as perfect electric conductors. A number of 14 receiving nodes were placed in these cubicles, while the ambient noise signals are generated by 14 sources placed at the outer wall of the room. At both sides the antennas are placed at an height of 1 m. Fig. 4 shows a 2-D map of the simulated environment as well as the positions of the receivers and sources. A

rough model for the human body as a rectangular parallelepiped has been used. For the human body a classic two-thirds muscle homogeneous model [23], [24] has been used to get realistic values. The time variance of the channel has been modeled by randomly placing ten persons in the scenario in 100 different realizations. The relative dielectric permittivity ε_r was set to 9 for concrete walls, and 35.2 for the human body, while the conductivity σ was set to 0.06 and 1.16, respectively.

B. Radio Channel Measurements

In this paper we use channel measurements obtained during the Stanford July 2008 Radio Channel Measurement Campaign. More details on the full campaign can be found in [14]. In this appendix, we briefly summarize the most important features of the measurement setup.

1) Environment: To provide good input data for our localization algorithms, we set up the test environment as shown in Figure 10. We took measurements in a cubicle-style office environment with rich scattering due to the metallic frames of the cubicles and highly reflective walls. The room size was around 34 m $\times$ 12 m. Eight receivers were placed in two squares, while the transmitters were positioned at the outer walls. To simulate real time-variant environments, people were moving in the room while the measurements were being recorded.

2) Measurement Equipment: The measurements were taken with the RUSK Stanford channel sounder at a center frequency of 2.45 GHz with a bandwidth of 240 MHz, and a test signal length of 3.2 μs. The transmitter output power of the sounder was 0.5 W. A rubidium reference in the transmit (Tx) and receive (Rx) units ensured accurate timing and clock synchronization. The sounder used fast 1 $\times$ 8 switches at both transmitter and receiver, enabling switched-array MIMO channel measurements of up to 8 $\times$ 8 antennas, i.e. 64 links. The Tx and Rx antennas were off-the-shelf WiFi antennas, which were connected to the switches of the sounder units using long low-loss cables.

The full 8 $\times$ 8 channel was sounded every 100.76 ms. We recorded a total of $T = 1200$ samples, capturing the time variations of the channel. By proper calibration, we removed the RF effects of the equipment and of the cables so that the resulting data only contains the impulse responses of the channels, denoted as $h_{kl}(t, \tau)$.

REFERENCES

[1] J. Chen, K. Yao, and R. Hudson, "Source localization and beamforming," *Signal Processing Magazine, IEEE*, vol. 19, no. 2, pp. 30–39, Mar 2002.

[2] N. Patwari, J. Ash, S. Kyperountas, I. Hero, A.O., R. Moses, and N. Correal, "Locating the nodes: cooperative localization in wireless sensor networks," *Signal Processing Magazine, IEEE*, vol. 22, no. 4, pp. 54–69, July 2005.

[3] J. A. Costa, N. Patwari, and A. O. H. III, "Distributed weighted multidimensional scaling for node localization in sensor networks," *ACM Transactions on Sensor Networks*, vol. 2, no. 1, pp. 39–64, February 2006.

[4] C. Hoene and J. Willmann, "Four-way toa and software-based trilateration of ieee 802.11 devices," in *IEEE 19th International Symposium on Personal, Indoor and Mobile Radio Communications, 2008. PIMRC 2008.*, Sept. 2008, pp. 1–6.

[5] D. Humphrey and M. Hedley, "Super-resolution time of arrival for indoor localization," in *IEEE International Conference on Communications, 2008. ICC '08.*, May 2008, pp. 3286–3290.

[6] Z. Low, J. Cheong, C. Law, W. Ng, and Y. Lee, "Pulse detection algorithm for line-of-sight (los) uwb ranging applications," *Antennas and Wireless Propagation Letters, IEEE*, vol. 4, pp. 63–67, 2005.

[7] S. Galler, W. Gerok, J. Schroeder, K. Kyamakya, and T. Kaiser, "Combined aoa/toa uwb localization," in *Communications and Information Technologies, 2007. ISCIT '07. International Symposium on*, Oct. 2007, pp. 1049–1053.

[8] H. Lim, L.-C. Kung, J. C. Hou, and H. Luo, "Zero-configuration, robust indoor localization: Theory and experimentation," in *INFOCOM 2006. 25th IEEE International Conference on Computer Communications. Proceedings*, April 2006, pp. 1–12.

[9] M. Nezafat, M. Kaveh, and H. Tsuji, "Indoor localization using a spatial channel signature database," *Antennas and Wireless Propagation Letters, IEEE*, vol. 5, no. 1, pp. 406–409, Dec. 2006.

[10] J. Garnier and G. Papanicolaou, "Passive sensor imaging using cross correlations of noisy signals in a scattering medium," *SIAM Journal on Imaging Sciences*, vol. 2, pp. 396–437, 2009.

[11] L. Stehly, M. Campillo, B. Froment, and R. L. Waver, "Reconstructing Green's function by correlation of the coda of the correlation (C^3) of ambient seismic noise," *Journal of Geophysical Research*, vol. 113, pp. 1–10, 2008.

[12] W. S. Torgerson, "Multidimensional scaling: I. theory and method," *Psychometrika*, vol. 17, no. 4, pp. 401–419, 1952.

[13] J. C. Gower, "Some distance properties of latent root and vector methods used in multivariate analysis," *Biometrika*, vol. 53, no. 3 and 4, pp. 325–338, 1966.

[14] N. Czink, B. Bandemer, G. Vazquez-Vilar, L. Jalloul, and A. Paulraj, "Stanford July 2008 radio channel measurement campaign," Stanford University, presented at COST 2100, TD(08)620, Lille, France, Tech. Rep., October 2008.

[15] P. Roux, K. G. Sabra, W. A. Kuperman, and A. Roux, "Ambient noise cross correlation in free space: Theoretical approach," *J. Acoust. Soc. Am.*, vol. 117, no. 1, pp. 79–84, 2005.

[16] R. Snieder, "Extracting the green's function from the correlation of coda waves: A derivation based on stationary phase," *Physical Review E*, vol. 69, 2004.

[17] J. de Leeuw, *Recent Developments in Statistics*, J. Barra and F. B. andG. Romier andB. Van Cutsem, Eds. Amsterdam: North Holland Publishing Company, 1977.

[18] K. Langendoen and N. Reijers, "Distributed localization in wireless sensor networks: a quantitative comparison," *Computer Networks*, vol. 43, pp. 499–518, 2003.

[19] S. Berger and A. Wittneben, "Carrier phase synchronization of multiple distributed nodes in a wireless network," in *8th IEEE Workshop on Signal Processing Advances for Wireless Communications (SPAWC), Helsinki, Finland*, June 2007.

[20] C. Oestges, B. Clerckx, L. Raynaud, and D. Vanhoenacker-Janvier, "Deterministic channel modeling and performance simulation of microcellular wide-band communication systems," *IEEE Trans. Veh. Technol.*, vol. 51, no. 6, pp. 1422–1430, November 2002.

[21] F. Mani and C. Oestges, "Evaluation of diffuse scattering contribution for delay spread and crosspolarization ratio prediction in an indoor scenario," in *4th European Conference on Antennas and Propagation - EuCAP*, Barcelona, Spain, April, 12-16 2010.

[22] V. DegliEsposti, F. Fuschini, E. M. Vitucci, and G. Falciasecca, "Measurement and modelling of scattering from buildings," *IEEE Trans. Antennas Propagat.*, vol. 55, no. 1, pp. 143–154, January 2007.

[23] A. Ruddle, "Computed sar levels in vehicle occupants due to on-board transmissions at 900 mhz," in *Antennas Propagation Conference, 2009. LAPC 2009. Loughborough*, Nov. 2009, pp. 137 –140.

[24] P. S. Hall and Y. Hao, *Antennas and propagation for body-centric wireless communications*. Artec House,London, 2006.

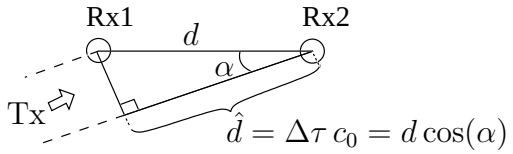

Fig. 1. A plane wave from a single source is observed with a specific delay at both receivers. The delay difference is used to estimate the distance between the receivers.

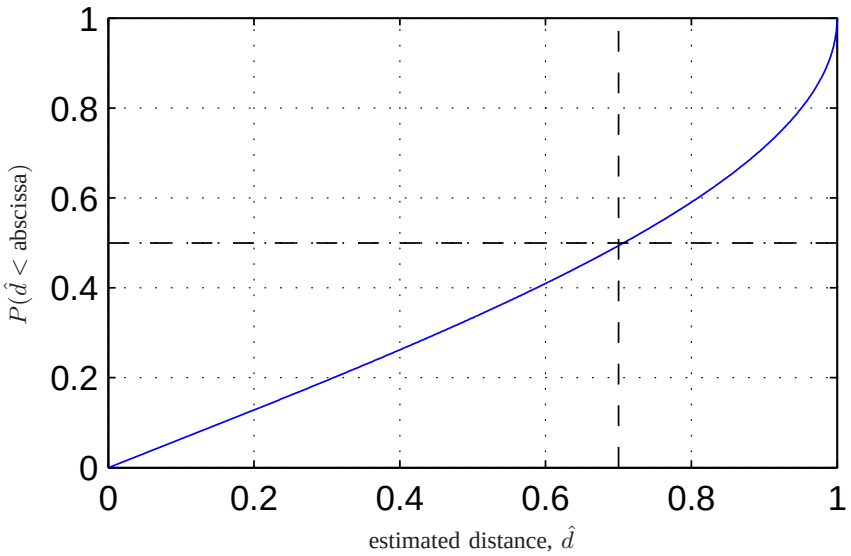

Fig. 2. Cumulative distribution function of $\hat{d}$ for $d = 1$, assuming a uniform distribution of the direction of the impinging wave. In 50% of the the cases the estimation error is less than 30%.

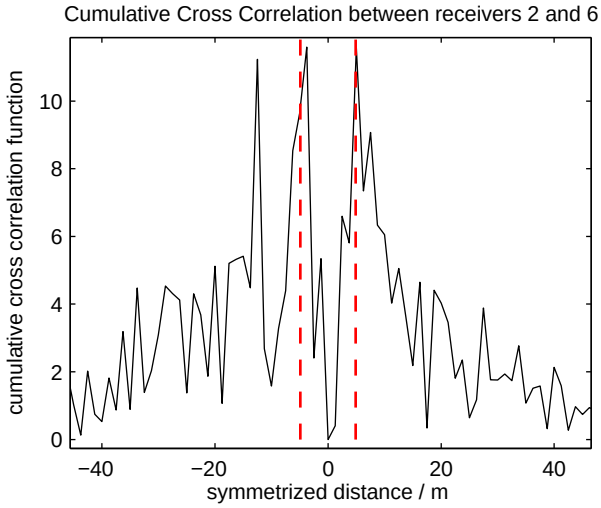

Fig. 3. A cross correlation function computed from our data (between receiving nodes 2 and 6). The true distance of 4.9 m is nicely reflected by the peaks.

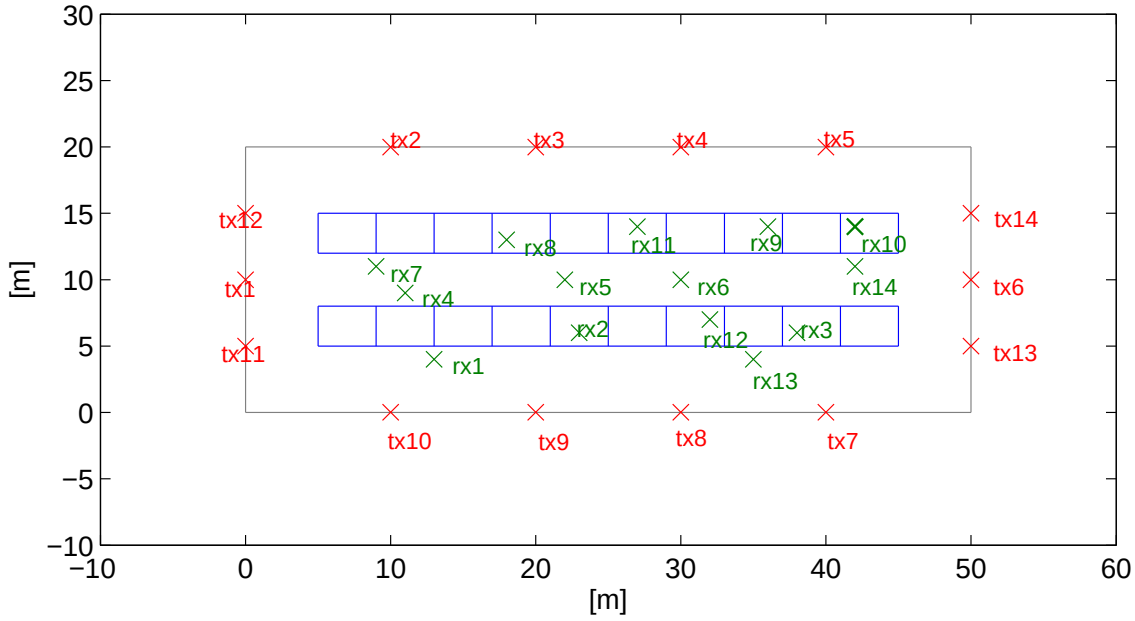

Fig. 4. Location of transmitters and receivers for simulations. The red x's are the transmitters around the perimeter are the transmitters and the green x's inside are the passive receivers. There are 14 of each. The scale is in meters.

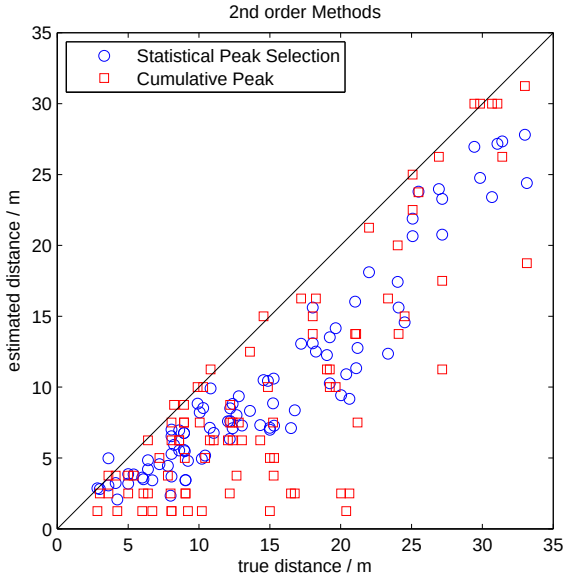

Fig. 5. Scatter plots of true distance versus estimated distance for different localization approaches. Notice the large underestimation bias.

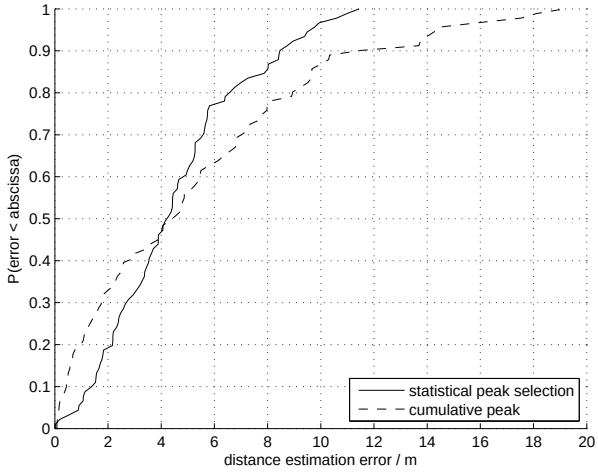

Fig. 6. CDF for pairwise distance estimation errors for each pair of receiver nodes, with two different correlation methods. The symbols differentiate between the different techniques to estimate the pairwise distance using cross correlations: weighted average of multiple peaks (“statistical peak selection”), and, for reference, the peak of the averaged long-time CCF (“cumulative peak”).

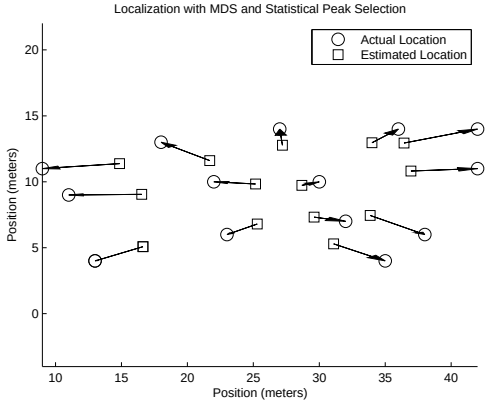

Fig. 7. Localization using our statistical peak selection method. The circles represent the true positions, while the squares represent the position estimates. The minimum localization error is 1.25 m, the maximum is 5.87 m, the average is 3.66 m, and the standard deviation is 1.56 m.

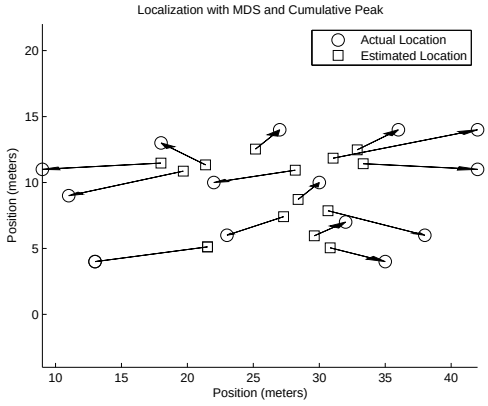

Fig. 8. Localization using the peak of the averaged long-time CCF.

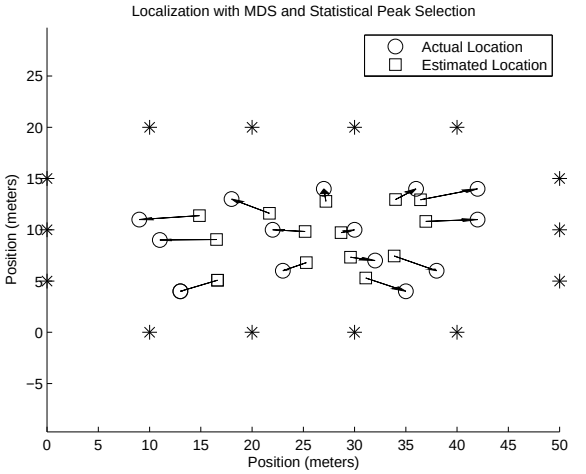

(a) Full

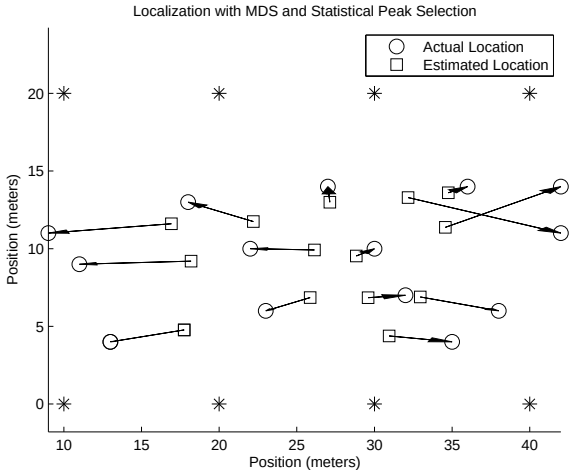

(b) Top and Bottom

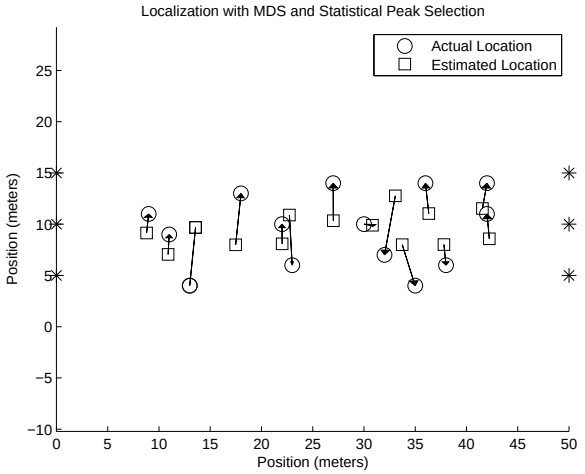

(c) Left and Right

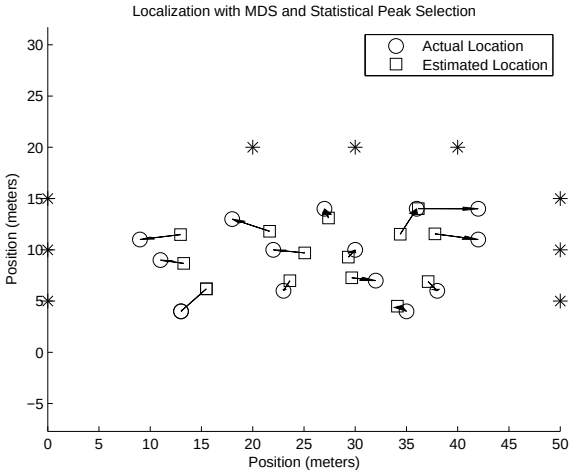

(d) Best

Fig. 9. Localization results from the simulated data with 4 different choices of transmitters are presented for different localization approaches. The asterisks denote the transmitter locations. (a) uses all the transmitters, (b) uses only the top and bottom transmitters, (c) uses only the left and right side transmitters, and (d) is the configuration found to gave the best location estimate (the search was not exhaustive).

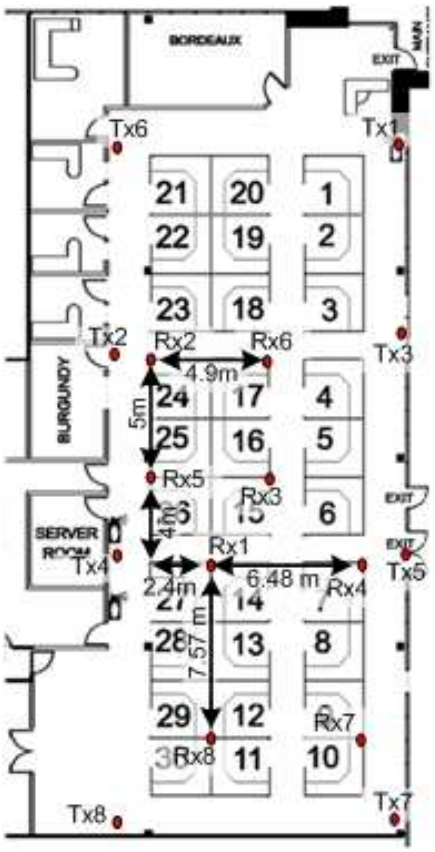

Fig. 10. Floor plan of the cubicle-style office environment used for the localization measurements. Rx1-Rx8 are the locations of the receiving nodes while Tx1-Tx8 are the locations of the antennas generating the ambient signals.

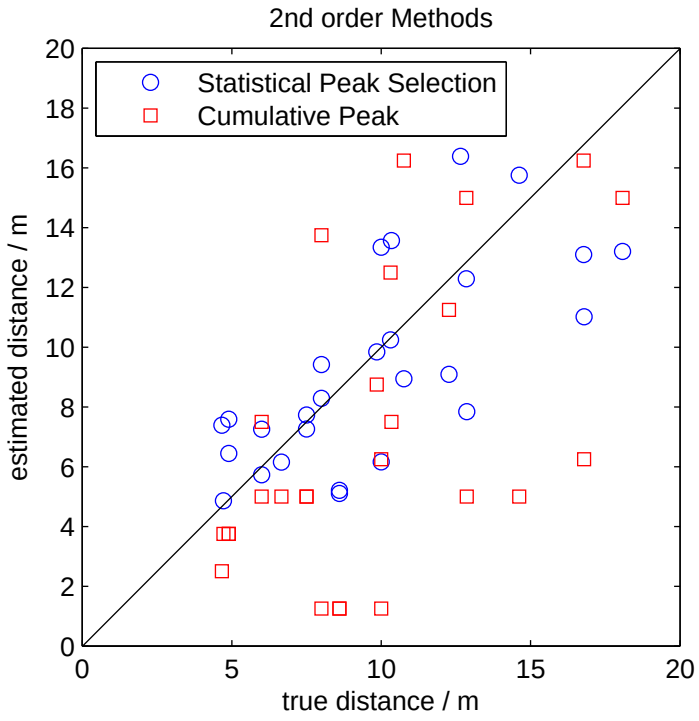

Fig. 11. Scatter plots of true distance versus estimated distance for different localization approaches.

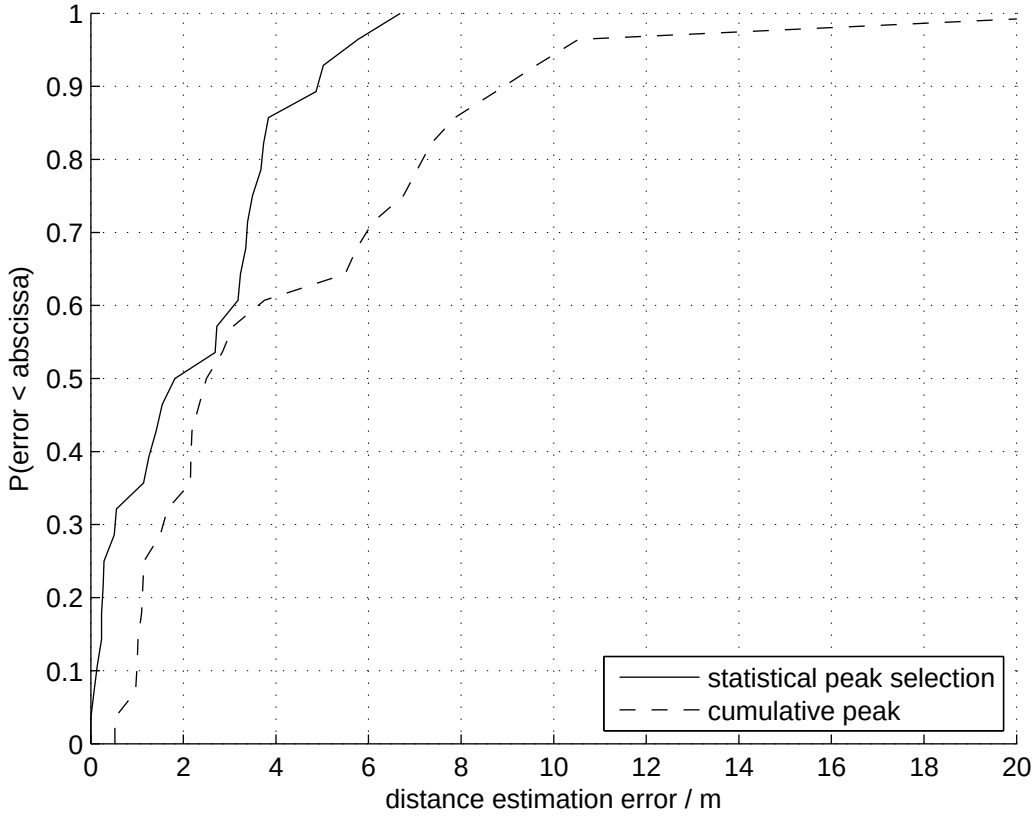

Fig. 12. CDF for pairwise distance estimation errors for each pair of receiver nodes, with two different correlation methods. The symbols differentiate between the different techniques to estimate the pairwise distance using cross correlations: weighted average of multiple peaks (“statistical peak selection”), and, for reference, the peak of the averaged long-time CCF (“cumulative peak”).

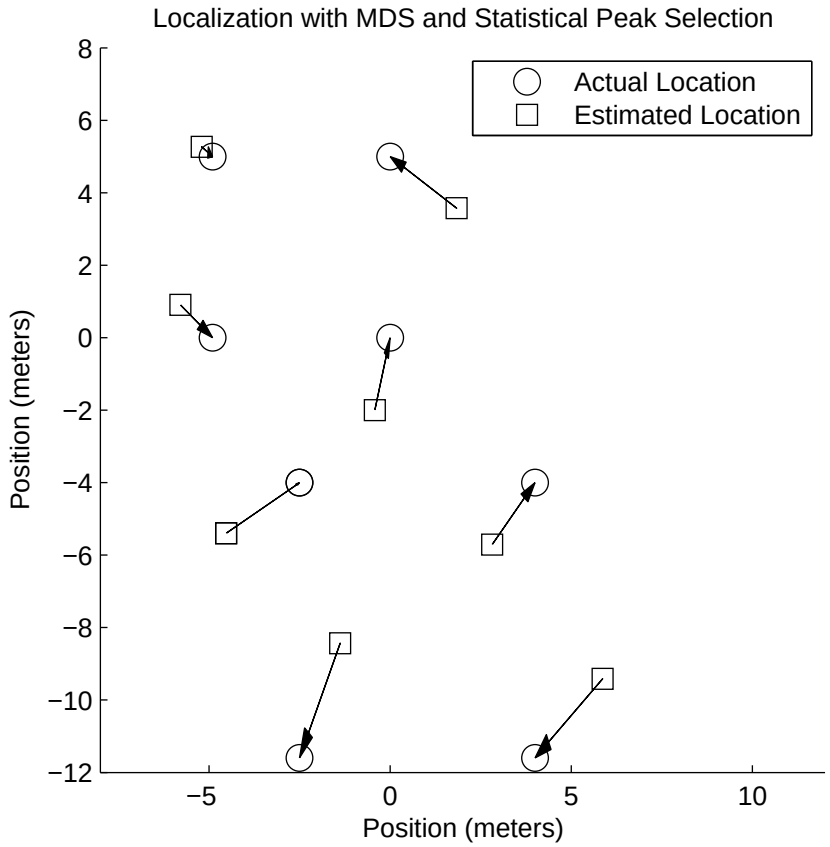

Fig. 13. Localization using our statistical peak selection method. The circles represent the true positions, while the squares represent the position estimates. The minimum localization error is 0.40 m, the maximum is 3.36 m, the average is 2.10 m, and the standard deviation is 0.92 m.

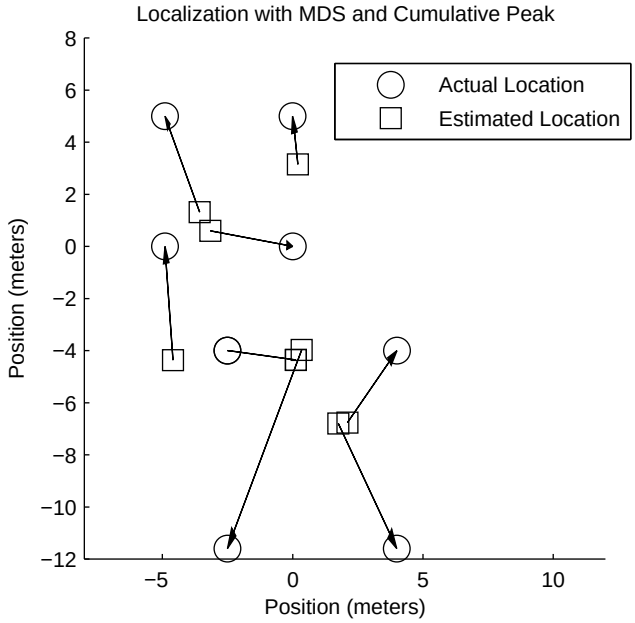

Fig. 14. Localization using the peak of the averaged long-time CCF. Localization is worse but not impossible when multipath is not exploited.